Numerical Simulation of Long-Term Effects of Weathering Due to Salt-Crystallization on Masonry Quay Walls

Alberto Gagliardi[1], Satyadhrik Sharma[2(✉)], Giovanni Castellazzi[1], and Rita Esposito[2]

[1] Department of Civil, Chemical, Environmental, and Materials Engineering, University of Bologna, Bologna, Italy
alberto.gagliardi2@studio.unibo.it

[2] Department of Materials, Mechanics, Management and Design, Delft University of Technology, Delft, The Netherlands
s.sharma-9@tudelft.nl

Abstract. Environmental factors, projected to intensify due to climate change predictions, can expedite the degradation and aging of historic building materials like masonry. Among the primary degradation risks, salt crystallization stands out. Historical masonry quay walls, a vital component of the infrastructure of numerous European cities, notably in the Netherlands, present a unique case study in this aspect. This uniqueness arises from their continuous and long-term exposure, not only to environmental influences but also to salts in the canal water. To investigate this, a coupled multiphase modeling strategy for the hygrothermal analysis of masonry structures is used to simulate the impact of salt crystallization on multi-wythe masonry quay walls in the city of Amsterdam. This modeling strategy is governed by four highly nonlinear and fully coupled differential equations addressing moisture mass conservation, salt mass conservation, energy balance, and salt crystallization/dissolution kinetics. The model has been previously validated against laboratory experiments, but it is here applied for the first time to a real case study. A parametric study adopting a 2D sectional numerical model of the quay wall was performed. Parameters investigated include the effects of boundary conditions at different faces of the quay wall, masonry bond pattern, salt concentration in the water as well as time variance of environmental relative humidity. The findings of this paper can be used to identify critical environmental conditions for quay walls as well as provide the basis for explaining the through-thickness variation of mechanical properties found in previous research.

Keywords: Unreinforced brick masonry · urban infrastructure · coupled multiphase modeling · salt-crystallization

G. Milani and B. Ghiassi (Eds.): IB2MaC 2024, LNCE 613, pp. 820–832, 2024.
https://doi.org/10.1007/978-3-031-73314-7_63

1 Introduction

Urban masonry infrastructures, such as bridges and quay walls, are currently in need of maintenance in several Dutch cities. This infrastructure often represents the main transportation system in city centers, both on land and water, as well as a historical asset (Fig. 1). Besides the increase of anthropogenic hazard, i.e. higher traffic load, climate-change effects can represent a relevant cause for the mechanical degradation of masonry with consequences on structural safety. Among others the increase in temperature may lead to a salinization of the waters in the canals, triggering salt-crystallization damage in the masonry.

Preliminary investigations have shown a through-thickness variation of mechanical properties, which may become relevant for the assessment of the remaining service life of this infrastructure. Xi and Esposito [10] performed mechanical characterization tests for a bridge in the city of Amsterdam. They reported that the masonry close to the waterside showed higher values of elastic modulus and lower values of flexural bond properties concerning masonry inside the structure; additionally, no variation of compressive strength was found. This may indicate the presence of degradation and/or aging mechanisms.

To understand the long-term effects of weathering due to salt-crystallization on masonry urban infrastructures, a coupled multiphase model is used as a case study of a quay wall in the city of Amsterdam. The case study is representative of quay walls in the inner city, also listed as a UNESCO heritage site, and represents one of the most vulnerable typologies currently identified. 2D sectional hygro-thermal analyses are carried out considering the model proposed in [3]. This approach can account for the coupling between moisture mass conservation, salt mass conservation, energy balance, and salt crystallization/dissolution kinetics. The model has been extensively validated against laboratory tests [3,5,6] and it is here applied to the analyses of a real case study.

The paper presents first a brief overview of the modeling approach in Sect. 2 and a description of the case study in Sect. 3. In Sect. 4, numerical results are presented and discussed considering the influence of masonry texture and the variation of relative humidity in time. Concluding remarks are presented in Sect. 5.

2 Coupled Multiphase Modeling of Masonry

In this section, the coupled multiphase model developed and presented in [3] is briefly recalled and utilized to simulate hygroscopic phenomena, salt transport, and crystallization in masonry structures exposed to weather conditions.

In this modeling approach, a porous material is conceived as a multiphase continuous porous medium, which represents a system of pores within a solid matrix. The pores can be (partially) filled with a liquid phase, a gaseous phase and precipitated/crystallized salts. In general, the multiphase continuous porous medium could be constituted by three different species: (i) the material matrix (solid phase), (ii) the water (gaseous phase and liquid phase), and (iii) the salt

Fig. 1. Quay wall in Amsterdam.

(liquid phase and solid phase). Isothermal conditions are considered. Only one salt is supposed in the solution and, although several salt solid phases can be implemented in the model, as carried out in [5], only one salt solid phase is herein considered. Furthermore, the concentration of liquid water can be generally approximated by the concentration of moisture to keep the model simple [3].

The multiphase porous medium is formulated based on three governing equations. Particularly, the moisture mass conservation equation (Sect. 2.1), the salt mass conservation equation (Sect. 2.2), and an evolution equation (Sect. 2.3), describing the salt precipitation/dissolution kinetics, are conceived. Three independent primary variables govern the multiphysics phenomena: (i) the pore relative humidity h (defined as the ratio between the actual vapor pressure and the vapor pressure at saturation), (ii) the mass fraction of the dissolved salt ω (kg/kg), (iii) and the concentration of solid salt per unit volume of porous medium c_s^s (kg/m^3). The content of each component is provided by the concentration c_α^π, defined as the mass of the specie α in π-phase (m_α^π) per unit volume of the porous medium, and by the saturation degree S_α^π, defined as the pore volume occupied by the specie α in π-phase.

2.1 Moisture Mass Conservation

The moisture mass conservation can be written as:

$$\frac{\partial c_w}{\partial t} + \nabla \cdot \mathbf{j}_w = 0 \tag{1}$$

where c_w is the concentration of moisture, $\mathbf{j}_w$ is the water flux (i.e., the sum of water vapor $\mathbf{j}_w^g$ and liquid $\mathbf{j}_w^l$ fluxes), and the operator $\frac{\partial}{\partial t}$ represents a time derivative.

2.2 Salt Mass Conservation

The salt mass conservation can be written as:

$$\frac{\partial c_s^l}{\partial t} + \nabla \cdot \mathbf{j}_s^l + \frac{\partial c_s^s}{\partial t} = 0 \tag{2}$$

where c_s^l is the concentration of liquid salt and $\mathbf{j}_s^l$ is the flux of dissolved salt. Furthermore, the expressions for $\mathbf{j}_w^l$ and $\mathbf{j}_s^l$ are:

$$\mathbf{j}_w^l = (1-\omega)\mathbf{j}_{ws}^l - \mathbf{j}_{s,diff}^l \tag{3}$$

$$\mathbf{j}_s^l = \omega \mathbf{j}_{ws}^l - \mathbf{j}_{s,diff}^l \tag{4}$$

where $\mathbf{j}_{ws}^l$ is the flux of the liquid phase and $\mathbf{j}_{s,diff}^l$ is the diffusive flux of the dissolved salt.

2.3 Evolution Equation

The salt crystallization or dissolution is assumed to be governed by the supersaturation ratio $\omega/\omega_{\text{sat}}$, i.e. the ratio between the current concentration of dissolved salt ω and the concentration at saturation ω_{sat}. Crystallization starts when the supersaturation ratio is greater than the threshold α_0, and dissolution starts when the supersaturation ratio is less than one:

$$\frac{\omega}{\omega_{\text{sat}}} = \begin{cases} > \alpha_0 \; crystallization \\ < 1 \quad dissolution \end{cases}$$

For primary crystallization, $\alpha_0 > 1$ then proceeds at $\alpha_0 = 1$. The specific values of α_0 to trig the primary crystallization depends on the nature of the porous media and the kind of salt (i.e. could be up to 1.7 in the case of red brick and NaCl salt [7]). Here, we adopt a unit value also for the threshold of supersaturation ratio for primary crystallization. This value is used also in the following evolution equation that is used to describe the salt precipitation/dissolution kinetics, which quantifies the amount of salt precipitated, can be written as:

$$\frac{\partial c_s^s}{\partial t} = \pi r_p^2 \rho_s^s \frac{n}{V_{tot}} K_c \left| \frac{\omega}{\omega_{sat}} - 1 \right|^P \tag{5}$$

In Eq. (5), c_s^s is measured in $[kg/m^3]$ and a constant amount of salt nuclei n in the solution is assumed, as well as an isotropic distribution of cylindrical pores and cylindrical nuclei of the same radius of the pores (r_p). Here, ρ_s^s represents the density of the crystallized salt, K_c is the growth rate coefficient, ω_{sat} denotes the concentration of dissolved salt at saturation, V_{tot} the pore volume, and P stands for the order of the crystallization process, see [3].

2.4 Constitutive Equations

The following constitutive equations are adopted to define the gas flow, the capillary liquid flow, and the diffusive flux of dissolved salt, respectively whose measure is provided in $(kg/m^2/s)$:

$$\mathbf{j}_w^g = -K_g \nabla p_v \tag{6}$$

$$\mathbf{j}_{ws}^l = -K_l \nabla p_c \tag{7}$$

$$\mathbf{j}_{s,diff}^l = -\rho_{ws}^l K_s \nabla \omega \tag{8}$$

where K_g is the vapor permeability, K_l the liquid permeability of the salt solution, K_s the salt diffusion coefficient, p_v the vapor pressure, p_c the capillary pressure, and ρ_{ws}^l the mass density of the liquid phase.

Here, for the sake of brevity, we recall briefly that the effect of salt precipitation on the gas and liquid conductivity is accounted automatically by changing the expressions of K_g and K_l using correcting functions (g_g and g_l, respectively) which depends on the effective porosity ϕ_{eff}:

$$K_g \leftarrow g_g\left(\phi_{eff}\right) K_g, \quad K_l \leftarrow g_l\left(\phi_{eff}\right) K_l \tag{9}$$

being

$$\phi_{eff} = \phi_0\left(1 - S_s^s\right) \tag{10}$$

where ϕ_0 is the initial porosity and S_s^s the saturation degree of crystallized salt, the interested reader could refer to [3,4,6]. Analogously to [9], the simple assumption of $g_g = g_l = 1 - S_s^s$ is made. Finally, the value of the salt diffusion coefficient K_s should depend on the actual cross-section available for diffusion. By taking this into account, K_s is assumed to be dependent on the saturation degree of the solution S_{ws}^l, i.e. its definition becomes:

$$K_s \leftarrow K_s \bullet S_{ws}^l \tag{11}$$

The vapor pressure and the capillary pressure in (6) and (7), respectively, can be expressed as:

$$p_v = p_{v,sat} h \tag{12}$$

$$p_c = \rho_w^l R_v T \ln(h) \tag{13}$$

where $p_{v,sat}$ is the saturation vapor pressure of the salt mixture, which depends on the temperature and the dissolved salt concentration, and ρ_w^l is the mass density of liquid water. In particular, for the calculation of the saturation vapour pressure of salt mixture the reader could refer to [5].

2.5 Boundary Conditions

The model formulation is completed by the initial boundary conditions. They can be of Dirichlet's type:

$$h = \overline{h} \tag{14}$$

$$\omega = \overline{\omega} \tag{15}$$

and of Neumann's or Robin's type:

$$\mathbf{j}_w \cdot \mathbf{n} = q_w + \gamma_w (A_w h - h_\alpha) \tag{16}$$

$$\mathbf{j}_s^l \cdot \mathbf{n} = q_\omega \tag{17}$$

Here, $\mathbf{n}$ represents the outward unit normal to the boundary, $\overline{h}$ and $\overline{\omega}$ are the prescribed humidity and salt concentration, respectively, q_w and q_ω are the prescribed normal fluxes of moisture and salt, respectively, h_α is the prescribed environmental humidity, A_w denotes the water activity, and γ_w is the convective humidity coefficient.

3 Case Study

3.1 Introduction to the Case Study

The case study refers to the *Marnixkade* quay, whose construction dates back to the end of the 19th, making it approximately 130 years old. It is located along the *Singelgracht* canal, in the North-West side of Amsterdam.

The quay consists of a masonry retaining wall topped with a granite capstone, built on a wooden pile foundation whose elements are connected by wooden beams. In [11] it was chosen as a case study due to a detailed inspection conducted in 2016, in which the data used in the following were gathered.

The altimetric values refer to the *Normaal Amsterdams Peil (NAP)*, used to indicate the average sea level in the North Sea and serves as a reference for elevations in the Netherlands, including the city of Amsterdam. Consequently, the portion of the wall submerged in the canal is approximately 0.6 m, leaving the remaining 0.8 m above the water (Fig. 2).

3.2 Boundary Conditions

The boundary conditions applied to the model to represent the surrounding environment, represented in Fig. 3 are of Dirichlet's type and Neumann's or Robin's type.

- Wet surface: Dirichlet's type boundary condition to reproduce the immersion in saline solution, i.e. $h = 100\%$, $\omega = 4\%$. Applied to the wall portions in direct contact with the water and the timber floor, which is assumed to be completely wet.

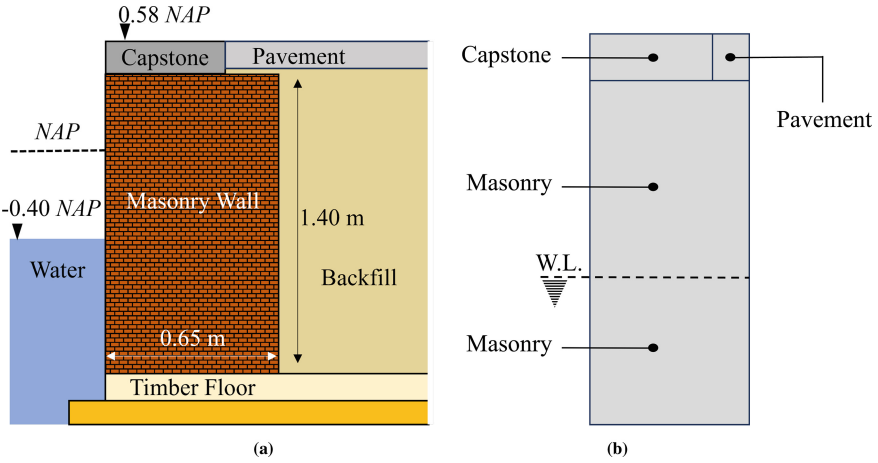

Fig. 2. General view of the quay wall section (a), masonry wall schematization (b) (adapted from [11]).

The dissolved salt concentration (ω) in the canal's water is assumed to be 4 grams per liter ($\omega = 4\%$), see [3]. This concentration value, used to speed up the following analyses, is higher than what is monitored in Amsterdam, see [12]. However, it is possible that the quay walls in Amsterdam have been exposed to such salt concentration historically and quay walls in other parts of the Netherlands might be still exposed to similar salt concentrations.

– Evaporative surface: Neumann's type boundary condition, to reproduce the evaporation process on the exposed face of the wall.
  The relative humidity (RH) of the surrounding environment is the main parameter influencing the flux, i.e. kept constant at RH = 55%.
– Sealed surface: Neumann's type boundary condition to model a sealed surface, applied to the backfill and the wall-capstone interface due to their hygroscopic properties.

3.3 Homogeneous and Textured Models

To evaluate the relevance of masonry texture on the deterioration process, a model considering the masonry as homogeneous material (Fig. 4a) and a model including the texture of masonry (Fig. 4d) are compared.

The chosen mesh is a quadrangular mapped type for the homogeneous model (Fig. 4b) and a free triangular for the textured model (Fig. 4d).

Due to the lack of physical characterization of the material for the selected case study, material properties are assumed based on previous work considering similar fired red clay brick masonry [3]. A summary of the model parameters is shown in Table 1.

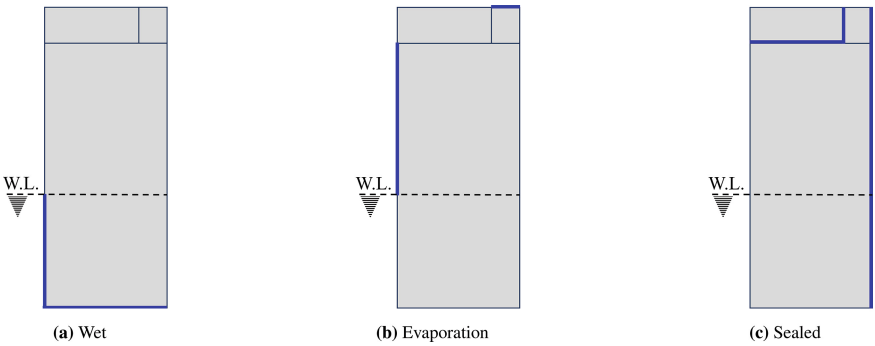

Fig. 3. Boundary conditions applied to the models.

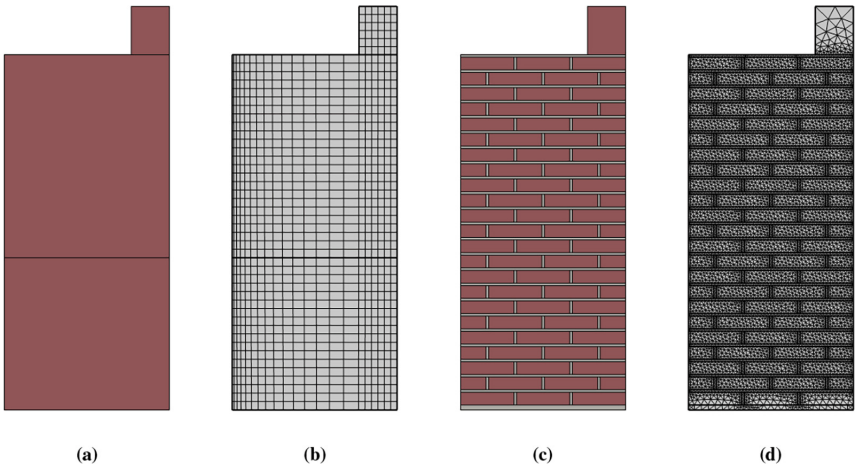

Fig. 4. Materials and meshes.

4 Influence of Masonry Texture on the Numerical Results

4.1 Steady State Solutions

The steady-state results of the homogeneous and textured model, reported in Fig. 5 show that the wall portion interested by the crystallization is wider in the textured model: the crystallized salt reaches a depth of about 4 cm in the homogeneous model, against the 13 cm of the textured model. Moreover, the $\omega/\omega_{\text{sat}}$ maps, show how the wall portion close to the crystallization threshold is considerably larger in the textured model.

The maximum amount of crystallized salt in the textured model reaches a value of $c_s^s = 540$ kg/m^3, a value very close to the saturation value (560 kg/m^3), and considerably higher than the maximum value reached by the homogeneous model of $c_s^s = 420$ kg/m^3.

Table 1. Summary of the model parameters

	Quantity	Value	Source
ω_{sat}	Concentration of dissolved salt at saturation	0.264 kg/kg	Refs. [1,3,9]
α_0	Crystallization threshold	1	Ref. [7]
ρ_s^s	Solid NaCl density	2160 kg/m^3	Literature
Brick			
r_b	Mean pore radius	0.700 [µm]	Ref. [3]
ϕ_0	Initial porosity	26.0%	Ref. [3]
A	Water adsorption coefficient	0.185 [kg/m^2/s$^{0.5}$]	Ref. [3]
K_s	Salt diffusion coefficient	0.499×10^{-9} [m^2/s]	Ref. [3]
CEM			
r_b	Mean pore radius	0.041 [µm]	Ref. [8]
ϕ_0	Initial porosity	22.5%	Ref. [8]
A	Water adsorption coefficient	0.05 [kg/m^2/s$^{0.5}$]	Ref. [8]
K_{s}	Salt diffusion coefficient	0.05×10^{-9} [m^2/s]	Ref. [2]

4.2 Evolution of the Phenomenon

The c_s^s developments over time, sampled from a cutpoint, taken 3 cm under the capstone and inside the wall from the canal side, is plotted in Fig. 6 for the homogeneous and textured models, show huge differences in terms of the development of the phenomenon.

The homogeneous model displays an activation phase of about 40 h of simulation, followed by a variation phase that reaches its steady-state solution after about 140 h. The maximum registered value of c_s^s registered in the cutpoint reaches 80 kg/m^3.

The textured model shows considerably dilated times, with an activation phase of about 160 h of simulation, followed by a variation phase that reaches its steady-state solution after about 600 h. The maximum registered value of c_s^s registered in the cutpoint reaches 350 kg/m^3, a much larger amount.

4.3 Long-Term Effects of Weathering

Long-term effects due to weathering can be simulated by varying environmental conditions due to seasonal cycles or daily temperature and humidity variations. In the case at hand, since NaCl salt is unaffected by temperature effects, the level of ambient humidity (RH) can be varied. In this preliminary work, this aspect is studied by sequentially placing three ideal conditions of ambient relative humidity, photographing the level of accumulated salt c_s^s downstream of three significant humidity variations that lead first to salt crystallization, then to salt dissolution, and subsequently to crystallization again. Therefore, three time intervals are considered: the first with RH = 55% which remains unchanged

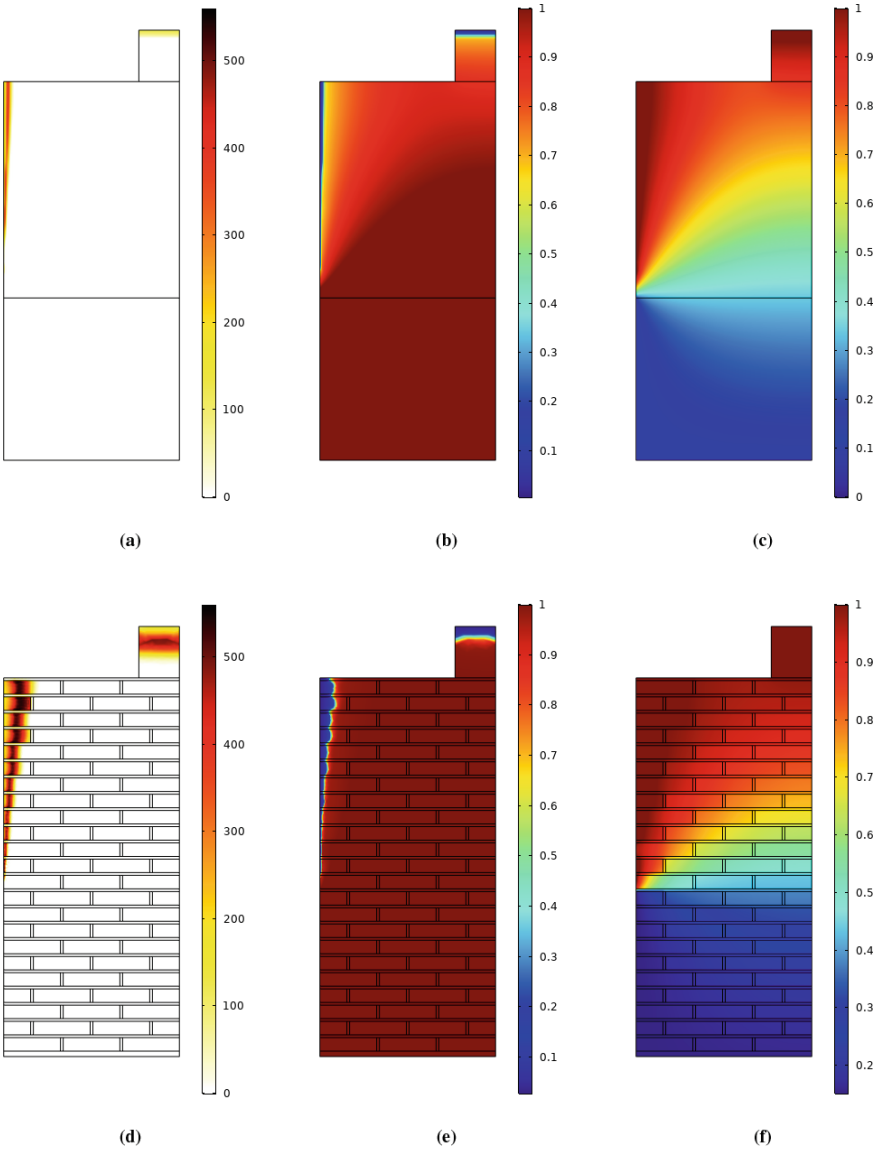

Fig. 5. Distribution maps of c_s^s, S_w^l and $omega/\omega_{\text{sat}}$ respectively for the homogeneous model (a, b, c) and the textured model (d, e, f).

for 300 h; the second with RH = 85% for 20 h, and the third with RH = 55% for 300 h. Inspecting Fig. 7, which shows the variation of c_s^s for these time instants, it can be noticed that the distribution of c_s^s depends on the sequence of events and not just on the time required to reach a steady state (see Fig. 6). Furthermore, it must be considered that this is only a preliminary analysis, meaning

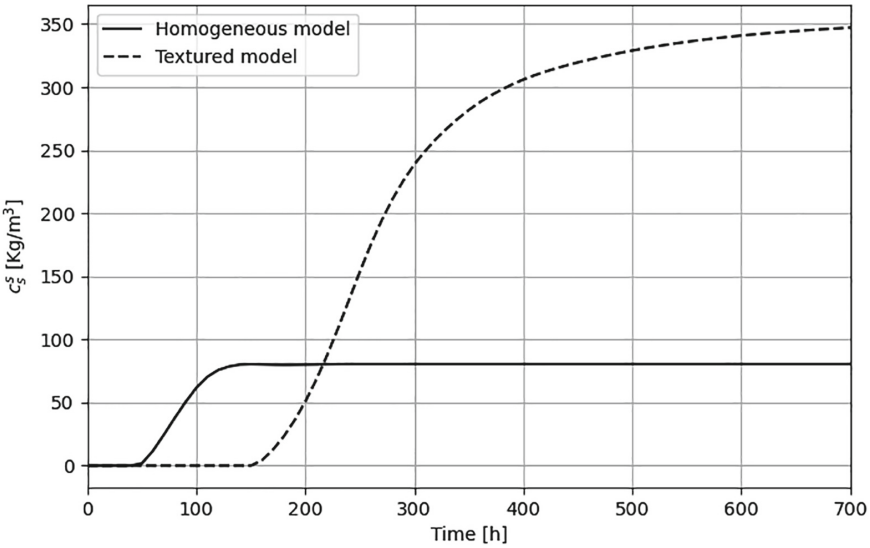

Fig. 6. Comparison of c_s^s evolution over time.

that potential variations in terms of porosity, tortuosity, and pore-filling degree caused by mechanical damage must be associated with this analysis [4].

A second cycle is carried out with the same RH values and runtimes.

5 Conclusions

In conclusion, the study presented a coupled multiphase modeling approach to analyze the impact of salt crystallization on multi-wythe masonry quay walls in Amsterdam, Netherlands. By incorporating highly nonlinear and fully coupled differential equations governing moisture mass conservation, salt mass conservation, energy balance, and salt crystallization/dissolution kinetics, the model provided valuable insights into the weathering effects experienced by historic masonry structures. Through a parametric study and numerical simulations, various factors such as material porosity, salt concentration in water, and masonry bond pattern were investigated. Additionally, the study explored the influence of masonry texture on numerical results, revealing differences in the approach to steady-state solutions between homogeneous and textured models. The brick-mortar texture was found to play a crucial role in the study of salt crystallization, with the textured model better reproducing conditions found in situ. Furthermore, the implementation of the bond pattern added complexity to the model, making convergence increasingly challenging. A future approach could involve tuning the homogeneous model to match the behavior of the textured model better, thus reducing computational load while maintaining accuracy. Overall, the findings contribute to advancing the understanding of weathering effects on

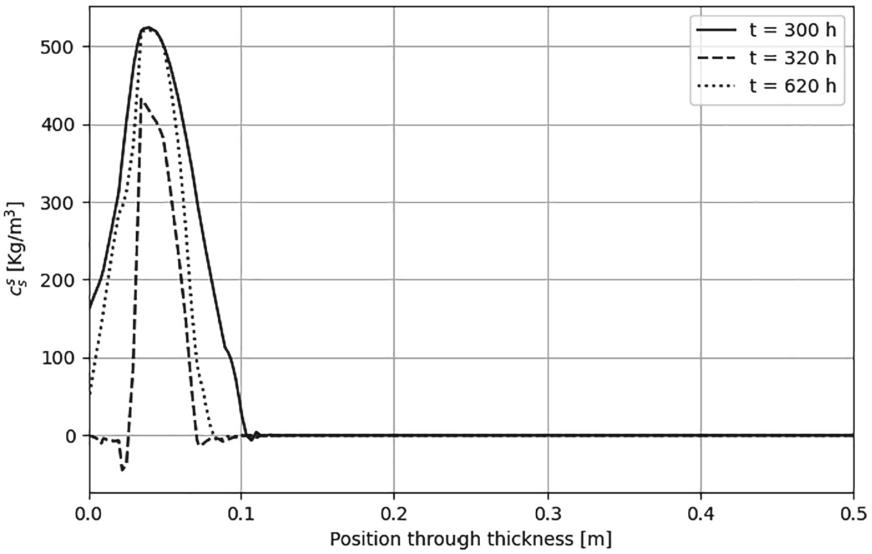

Fig. 7. Value of c_s^s along the wall thickness for the steady state and second weathering cycle.

historic masonry structures and aid in the development of effective preservation strategies to ensure their long-term durability and structural integrity. Moreover, this study underscores the significance of a numerical modeling approach in addressing real-world challenges and sheds light on the modeling of multiphysics phenomena in heritage conservation efforts.

Acknowledgments. This study was partially funded by the Amsterdam municipality through the Amsterdam Institute for Advanced Metropolitan Solutions (AMS), under the Bridges and Quay Walls Research Programme (Programma Bruggen en Kademuren).

References

1. Ahl J (2004) Salt diffusion in brick structures. Part II: The effect of temperature, concentration, and salt. J Mater Sci 39(13):4247–4254
2. Akrout K, Ltifi M, Ouezdou MB (2010) Chloride diffusion in mortars—effect of the use of limestone sand. Part II: Immersion test. Int J Concrete Struct Mater 4:109
3. Castellazzi G, Colla C, de Miranda S, Formica G, Gabrielli E, Molari L, Ubertini F (2013) A coupled multiphase model for hygrothermal analysis of masonry structures and prediction of stress induced by salt crystallization. Constr Build Mater 41:717–731
4. Castellazzi G, D'Altri AM, de Miranda S, Emami H, Molari L, Ubertini F (2021) A staggered multiphysics framework for salt crystallization-induced damage in porous building materials. Constr Build Mater 304:124486

5. Castellazzi G, de Miranda S, Grementieri L, Molari L, Ubertini F (2016) Multiphase model for hygrothermal analysis of porous media with salt crystallization and hydration. Mater Struct 49(3):1039–1063
6. de Miranda S, D'Altri AM, Castellazzi G (2019) Modeling environmental ageing in masonry strengthened with composites. Eng Struct 201:109773
7. Espinosa RM, Franke L, Deckelmann G (2008) Phase changes of salts in porous materials: crystallization, hydration and deliquescence. Constr Build Mater 22(8):1758–1773
8. Franzoni E, Santandrea M, Gentilini C, Fregni A, Carloni C (2019) The role of mortar matrix in the bond behavior and salt crystallization resistance of FRCM applied to masonry. Constr Build Mater 209:592–605
9. Grementieri L, Molari L, Derluyn H, Desarnaud J, Cnudde V, Shahidzadeh N, de Miranda S (2017) Numerical simulation of salt transport and crystallization in drying Prague sandstone using an experimentally consistent multiphase model. Build Environ 123:289–298
10. Li X, Esposito R (2023) A strategy for material characterisation of multi-wythe masonry infrastructure: preliminary study. Constr Build Mater 408
11. Sharma S, Longo M, Messali F (2023) A novel tier-based numerical analysis procedure for the structural assessment of masonry quay walls under traffic loads. Front Built Environ 9
12. Waternet. Water in kaart. https://www.waternet.nl/ons-water/oppervlaktewater/water-in-kaart